Separation Science and Technology
Publication details, including instructions for authors and subscription information:
http://www.informaworld.com/smpp/title~content=t713708471

MICROCHANNEL DEVICES FOR EFFICIENT CONTACTING OF LIQUIDS IN SOLVENT EXTRACTION

W. E. TeGrotenhuis[a]; R. J. Cameron[a]; M. G. Butcher[a]; P. M. Martin[a]; R. S. Wegeng[a]
[a] Pacific Northwest National Laboratory, Richland, Washington

To cite this Article TeGrotenhuis, W. E. , Cameron, R. J. , Butcher, M. G. , Martin, P. M. and Wegeng, R. S.(1999) 'MICROCHANNEL DEVICES FOR EFFICIENT CONTACTING OF LIQUIDS IN SOLVENT EXTRACTION', Separation Science and Technology, 34: 6, 951 — 974
To link to this Article: DOI: 10.1080/01496399908951075
URL: http://dx.doi.org/10.1080/01496399908951075

SEPARATION SCIENCE AND TECHNOLOGY, 34(6&7), pp. 951–974, 1999

MICROCHANNEL DEVICES FOR EFFICIENT CONTACTING OF LIQUIDS IN SOLVENT EXTRACTION

W. E. TeGrotenhuis, R. J. Cameron, M. G. Butcher,
P. M. Martin, and R. S. Wegeng
Pacific Northwest National Laboratory
Richland, Washington 99352

ABSTRACT

Microchannel devices were designed and tested for efficient contacting of two liquids in solvent extraction, and the results are presented. This study is part of an overall effort to produce and demonstrate efficient compact devices for chemical separations. Engineering these devices at the microscale offers many technical advantages. Achieving high contact area per unit system volume, thin-film contacting, and establishing uniform flow distribution result in substantially higher throughput per total system volume over conventional technologies. Theoretical calculations are presented that provide insight into the relative importance of various resistances to mass transfer, as well as their relationship to overall performance of the microchannel devices. Experimental results are presented for device performance using both commercial polymeric membranes and micromachined contactor plates for stabilizing the liquid-liquid interface. These results indicate that current-generation micromachined plates perform as well as commercial membranes, with substantial potential for improvement.

INTRODUCTION

Developments in microfabrication techniques, based on techniques founded in the electronics industry, are facilitating development of novel hardware for performing traditional chemical processing at a miniaturized scale (1). Features

are now designed with resolutions approaching 1–10 μm in microtechnology devices (2). At this scale, the distances for heat and mass transfer can be uniformly minimized, giving extremely rapid transport rates that result in very short residence times and high throughput per unit hardware volume (3,4). In addition, process conditions can be more tightly controlled. As all elements of traditional chemical processes are achieved using microtechnology, including heat exchangers (5), reactors (6), separators (7), and actuators (8,9), entire chemical processes can be miniaturized. The compact size enables distributed processing, which is particularly appealing for production of extremely hazardous or toxic chemicals to avoid the costs and risks associated with storage and transportation. Although traditional economies of scale in scaling up chemical processes are not as easily realized with microtechnology, the potential exists for economies of mass production (10,11) analogous to the dramatic reductions in manufacturing costs experienced in the microelectronics industry. The progress in developing microchemical separators for solvent extraction applications is described here.

Solvent extraction requires intimate contact of two immiscible liquids to facilitate mass transfer of one or more solutes from one fluid to another. Mixer-settler technologies accomplish this by dispersing one liquid into another followed by separation of the phases and recovery of the solvent. Although relatively mature as a technology, progress continues in the development of smaller, more efficient centrifugal contactors (12). An alternate approach is to contact the fluids as thin films. This can be done with an unconstrained fluid-fluid interface, such as that in extraction columns (13) or in microchannel devices (14), or with a support for immobilizing the interface, such as with membrane contactors (15). In all technologies, equipment size and operating costs are largely dictated by the capacity of the extractant and by mass transfer efficiency.

A novel approach for solvent extraction is under development based on microchannel devices. These devices resemble membrane contactors, but have

much greater versatility for substantially reducing mass transfer resistances, both in the flow streams and in the contactor plate. Film-contacting technologies offer advantages over more traditional mixer-settler technologies. One advantage is the ability to optimize the ratio of solvent flow to feed flow, which is generally minimized to reduce solvent recovery costs. The design of mixer-settlers becomes more difficult and mass transfer efficiency diminishes as the solvent-to-feed ratio becomes much less than one. Film contactors, on the other hand, can be designed and operated over a wide range of solvent ratios (15), which provides for more optimal use of solvent, especially when the equilibrium distribution coefficient for the solute is large. Furthermore, the effectiveness of each stage of a mixer-settler or a film contactor with a mobile interface is limited by equilibrium, and multiple stages are required to achieve a more effective separation. However, if the interface is immobilized, the two liquid films can flow in countercurrent directions, allowing for a more effective separation in a single device.

Microchannel devices are engineered at the microscale to achieve much higher heat and mass transfer rates than are found in macroscale technologies (1). These devices, when applied to solvent extraction, allow intimate contacting of two immiscible fluids as they flow through very thin channels that are smaller than the normal mass transfer boundary layer. By reducing the mass transfer resistances in each phase, overall mass transfer rates can be significantly enhanced and the overall size of the equipment reduced. The approach here is to use a microengineered support for the interface to allow countercurrent contacting while minimizing the mass transfer resistance in the support.

The architecture employed in this work consists of two micromachined channels separated by a contactor plate as shown in Figure 1. Devices can be operated cocurrently or countercurrently. The channels are separated by a micromachined contactor plate that has a matrix of uniform holes. A micrograph of a hole matrix is shown in Figure 2. The ability to stabilize the interface within

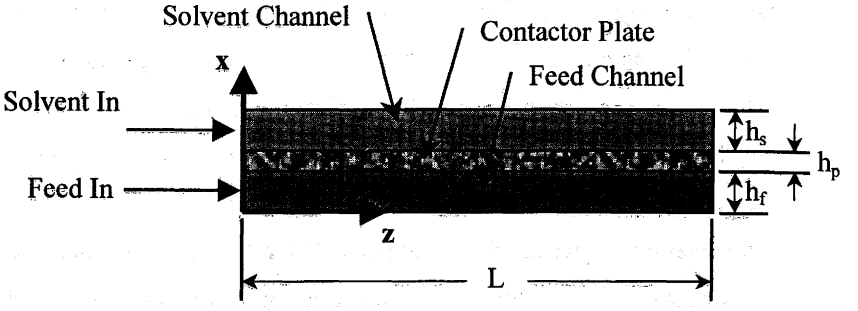

FIGURE 1. Microchannel contactor device geometry.

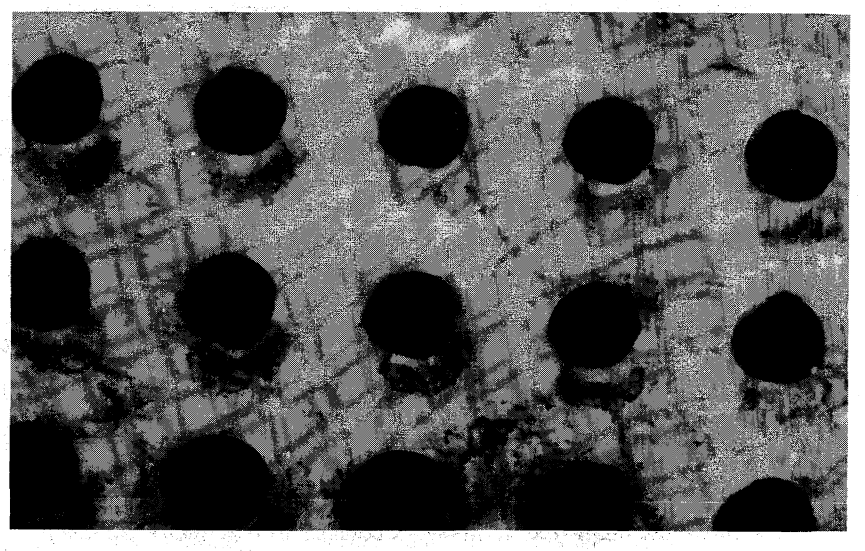

FIGURE 2. Micrograph of micromachined contactor plate fabricated from 1-mil (25-μm) Kapton substrate; holes are approximately 25 μm in diameter.

the contactor plate is governed by the Laplace equation (16), which dictates the maximum pressure drop across the contactor plate as

$$\Delta P = \frac{2\gamma \cos(\theta)}{r} , \qquad (1)$$

where γ is the liquid-liquid interfacial tension, θ is the contact angle, and r is the maximum hole size if the holes are round. Therefore, the pressures inside the device must be carefully controlled to prevent breakthrough of the fluids through the holes in the contactor plate.

The mass transfer resistance of the device has contributions from each flow stream, from the contactor plate, and from the interface. Interfacial mass transfer resistance can dominate, particularly if the extraction involves an interfacial reaction, such as that observed in the exchange of ions in the extraction of dissolved metals (17). If interfacial mass transfer resistance dominates, device performance is largely governed by the total interfacial surface area, and the thin, uniform flow channels in microchannel devices are not as great an advantage. The mass transfer resistance of the contactor plate is a function of several parameters, including the thickness of the contactor plate, porosity, tortuosity, and the solute diffusion coefficient in the wetting liquid that fills the pores (16). The objectives in this work are to reduce the overall size of the equipment and improve operating efficiency by (i) improving mass transfer efficiency in the flow channels by reducing the thicknesses of the films and (ii) improving mass transfer efficiency in the contactor plate. Here, the relative importance of mass transfer resistance in the flow channels versus the contactor plate is explored theoretically and experimentally, using both micromachined contactor plates and commercial polymeric membranes.

THEORY

The theoretical performance of a microchannel contactor having two immiscible fluids flowing through rectangular channels separated by a porous rigid plate can be determined by solving the convective-diffusion equation. Because the widths of the channels are much larger than the heights of the channels, the side-wall effects are neglected and the problem is reduced to two dimensions. The geometry is divided into three sections—the feed flow channel, the solvent flow channel, and the contactor plate—with equations written for each section. Boundary conditions allow the equations to be combined into a single mathematical model of the overall device. Dispersion in the flow direction is neglected in all three sections, while convection is neglected in the transverse direction, which is valid at low concentrations.

The flow fields are simple two-dimensional parabolic flow profiles, which, in the coordinate system depicted in Figure 1, results in the velocity profile

$$v_{f_z} = \frac{3}{2}\frac{Q_f}{W h_f}\left(\frac{4x}{h_f}\right)\left(1-\frac{x}{h_f}\right) \tag{2}$$

for the feed-side flow, where Q_f is the volumetric flow rate of the feed, W is the channel width, and h_f is the height of the feed flow channel. A similar velocity profile for the solvent side is

$$v_{s_z} = \frac{3}{2}\frac{Q_s}{W h_s}\left(1-\left(\frac{2\left(x-h^*\right)}{h_s}\right)^2\right), \tag{3}$$

where

$$h^* = h_f + h_p + \frac{h_s}{2} \quad ,$$

Q_s is the solvent volumetric flow rate, h_s is the height of the solvent flow channel, and h_p is the thickness of the contactor plate. For countercurrent flow, a negative sign is added to the left side of the equation.

Based on the assumptions stated above, the mass transfer differential equations are

$$v_{f_z} \frac{\partial c_f}{\partial z} = D_f \frac{\partial^2 c_f}{\partial x^2} \quad , \tag{4}$$

$$\frac{\partial^2 c_p}{\partial x^2} = 0 \quad , \tag{5}$$

$$v_{s_z} \frac{\partial c_s}{\partial z} = D_s \frac{\partial^2 c_s}{\partial x^2} \quad , \tag{6}$$

for the feed side flow, the contactor plate, and the solvent side flow, respectively, where c is solute concentration and D refers to solute diffusivity in the respective phases.

Six boundary conditions are required for the three second-order differential equations, which for the case of the solvent wetting and filling the contactor plate, are

$$\frac{\partial c_f}{\partial x} = 0 \qquad at \quad x = 0, \tag{7}$$

$$D_f \frac{\partial c_f}{\partial x} = k\left(c_f\big|_{x=h_f} - m_s \, c_p\big|_{x=h_f} \right) \qquad at \quad x = h_f, \tag{8}$$

$$D_e \frac{\partial c_p}{\partial x} = D_f \frac{\partial c_f}{\partial x} \qquad at \quad x = h_f, \tag{9}$$

$$c_p = c_s \qquad at \quad x = h_f + h_p, \tag{10}$$

$$D_s \frac{\partial c_s}{\partial x} = D_e \frac{\partial c_p}{\partial x} \qquad at \quad x = h_f + h_p, \tag{11}$$

$$\frac{\partial c_s}{\partial x} = 0 \qquad at \quad x = h_f + h_p + h_s, \tag{12}$$

where D_e represents an effective diffusion coefficient for the contactor plate that captures effects such as porosity and tortuosity. Equations (7) and (12) provide for zero flux through the solid channel walls. Equation (8) represents constant flux across the interface based on an interfacial mass transfer model. The parameter m_s is the equilibrium distribution coefficient, which is the ratio of feed concentration to solvent concentration at equilibrium, assumed to be constant over the concentration range in the device. The parameter k is a mass transfer coefficient representing the mass transfer resistance across the interface. Equation (9) assumes continuity of flux on both sides of the liquid-liquid interface, and Equations (10) and (11) represent continuity and constant flux at the contactor plate on the solvent side.

The initial conditions for cocurrent flow are

$$c_f = c_{f_0} \qquad at \quad z = 0, \tag{13}$$

$$c_p = c_s = 0 \qquad at \quad z = 0. \tag{14}$$

The differential equation for the contactor plate is solved analytically to give a linear concentration profile through the contactor plate. Therefore, the partial derivative of concentration in the contactor plate can be replaced by

$$\frac{\partial c_p}{\partial x} = \frac{\left(c_p\big|_{x=h_f+h_p} - \; c_p\big|_{x=h_f} \right)}{h_p} \tag{15}$$

in the boundary conditions above, and the differential equation for the plate, Equation (5), is eliminated.

The two convective-diffusion equations for the flow channels are solved numerically using the Crank-Nicholson (18) implicit method of finite differences, iterating from the feed end to the discharge end in sequential steps. The x-direction is nondimensionalized by the feed channel height, h_f, and concentrations are nondimensionalized by the feed initial concentration, c_{f0}. The z-direction is analogous to time and is nondimensionalized as

$$\tilde{z} = \frac{2}{3}\frac{D_f W}{Q_f h_f} z \,. \tag{16}$$

A Sherwood number is defined for the interfacial mass transfer using feed-side diffusivity and feed channel height for consistency,

$$\tilde{z} = \frac{D_f}{k h_f} \,. \tag{17}$$

The other two diffusivities, D_e and D_s, are scaled by the feed diffusivity, D_f. The interfacial boundary condition, Equation (8), becomes

$$Sh \frac{\partial \tilde{c}_f}{\partial \tilde{x}} = \tilde{c}_f\big|_{\tilde{x}=1} - \; m_s \, \tilde{c}_p\big|_{\tilde{x}=1} \qquad at \quad \tilde{x} = 1. \tag{18}$$

For most calculations reported here, the Sherwood number is assumed to be very small, representing very fast kinetics across the liquid-liquid interface. The other boundary conditions are similarly nondimensionalized.

The effluent concentration of a stream is calculated by averaging over the flow profile at the end of the channel, which for the feed stream becomes

$$c_{f_{eff}} = \frac{W}{Q_f} \int_0^{h_f} c_f(z = L)\ v_{f_z}\ dx . \tag{19}$$

This equation is nondimensionalized by the feed influent concentration as well.

From this point, all reported symbols and values are nondimensionalized unless otherwise noted, and the tilde is dropped.

Figures 3, 4, and 5 illustrate the theoretical dependence of effluent concentration on parameters affecting mass transfer efficiency. Feed and solvent flow rates are equal in all cases. For cocurrent flow, the curves form an asymptote to an effluent feed concentration that is in equilibrium with the solvent effluent concentration, as determined by mass balance of the solute. For example, if the equilibrium ratio, m_s, is 1.0 with equal flow rates, then the asymptote becomes 0.5, corresponding to equal effluent concentrations. This constraint on extraction efficiency is relaxed by countercurrent flow.

Figure 3 illustrates the sensitivity of the mass transfer efficiency to the effective diffusion coefficient for the contactor plate, D_e. Because the contactor plate is only one-twelfth the thickness of the flow channels, the contactor plate offers minimal mass transfer resistance when the contactor plate effective diffusivity is comparable to the bulk diffusivity. Increasing the effective diffusivity further has little impact on device performance. However, when the contactor diffusivity is an order of magnitude less than the bulk diffusivity, the contactor plate resistance dominates and the residence times required to reach equilibrium increase dramatically. This illustrates how the mass transfer resistance

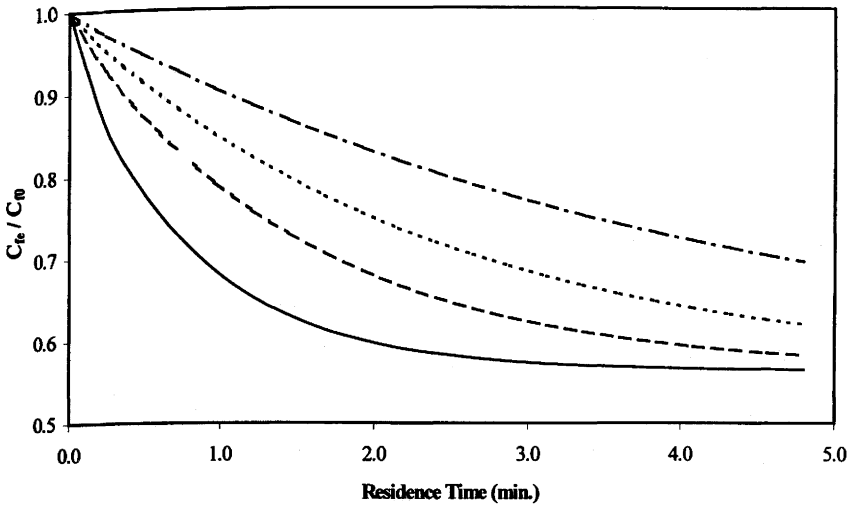

FIGURE 3. Effect of effective diffusion coefficient for the contactor plate on theoretical prediction of effluent solute concentration (normalized by feed concentration) when solvent and feed flow rates are equal for $D_e/D_f = 1.0$ (——), $D_e/D_f = 0.1$ (— —), $D_e/D_f = 0.05$ (- - -), and $D_e/D_f = 0.025$ (— - —), using $h_p/h_f = 1/12$, $m_s = 1.3$, $D_f = D_s$, and neglecting mass transfer resistance at the interface.

of the contactor plate is dependent on both the effective diffusivity and the plate thickness.

An important factor in evaluating device performance is accurately determining the equilibrium distribution coefficient, m_s, as illustrated by Figure 4. A relatively small error of 20% in the equilibrium distribution coefficient can cause the asymptote of the predicted curves to shift significantly, confounding efforts at determining the relative success in reaching optimal device performance. The final set of theoretical curves addresses the importance of interfacial mass transfer resistance. As expected, the mass transfer resistance of the interface does not become important until the Sherwood number approaches one, as shown in

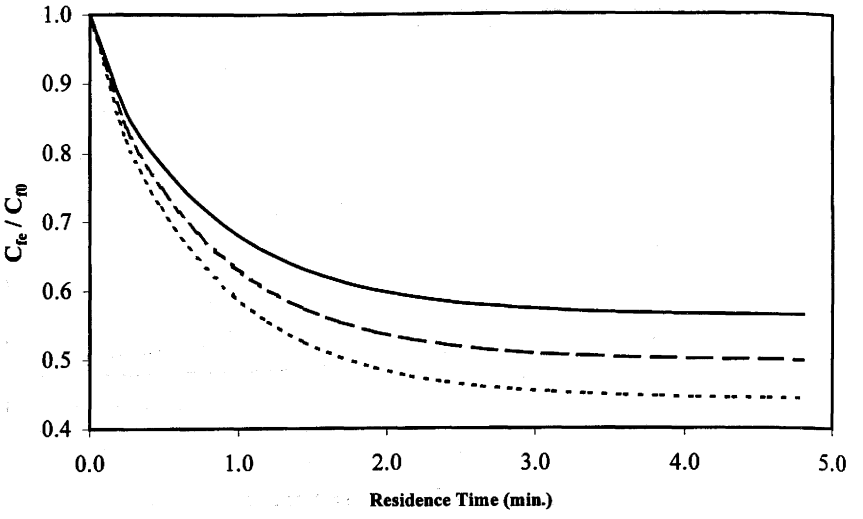

FIGURE 4. Effect of equilibrium distribution coefficient on theoretical prediction of effluent solute concentration (normalized by feed concentration) when solvent and feed flow rates are equal for $m_s = 0.8$ (—), $m_s = 1.0$ (— —), and $m_s = 1.3$ (- - -), using $h_p/h_f = 1/12$, $D_e = D_f = D_s$, and neglecting mass transfer resistance at the interface.

Figure 5. For the simple organic liquid system studied here, the Sherwood number is expected to be low and the interfacial resistance to be negligible.

EXPERIMENTAL PROCEDURES

Three types of experiments were performed in support of this investigation. In the first, equilibrium concentration ratios were measured over a range of total solute concentrations to quantify the equilibrium distribution coefficients for theoretical comparison. In the second, water and cyclohexane were run co-currently through the microcontactor device and the water effluent was measured for cyclohexane concentration. (The mass transfer resistance of the flow channel

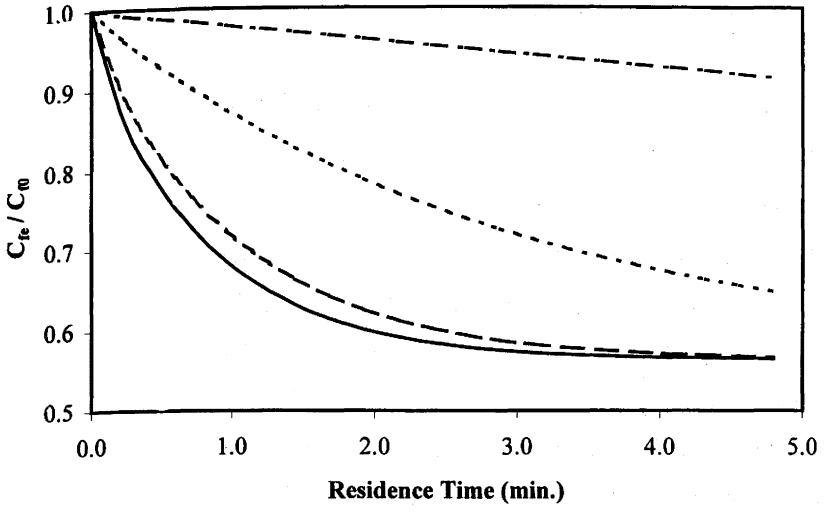

FIGURE 5. Effect of mass transfer resistance of the interface on theoretical prediction of effluent solute concentration (normalized by feed concentration) when solvent and feed flow rates are equal for Sh = 0.0003 (—), Sh = 0.3 (— —), Sh = 3 (- - -), and Sh = 30 (— - —), using $h_p/h_f = 1/12$, $D_e = D_f = D_s$, and $m_s = 1.3$.

was measured by itself in these experiments because the cyclohexane wets the contactor plates.) This allowed validation of the theoretical model for the flow channel mass transfer resistance. In the third set of experiments, cyclohexanol was added to the water stream and cyclohexane was used as the extractant. Although this is not necessarily a useful solvent extraction system, it serves the purpose of a model test system to evaluate and compare device performance.

Equilibrium distribution coefficient data were collected by mixing a stock solution of 1000 mg/L cyclohexanol in water with cyclohexane in various volume ratios. The mixtures were allowed to equilibrate over several hours. Samples were then taken from the water phase and analyzed by gas chromatography. The mixtures were then resampled and analyzed 24 hours later for comparison.

Two types of contactor plates were used in the microcontactor devices. Micromachined contactor plates were fabricated by laser drilling a matrix of holes through Kapton polymeric 1-mil and 2-mil (25-μm and 50-μm) film covering an area 1 cm wide by 8 cm long. In addition, experiments were performed with Gelman 3-μm Zefluor PTFE (Teflon) microporous membranes for comparison. Figure 2 gives an example of the structure of a micromachined contactor plate. The fabrication technique results in conical-shaped holes, with those shown in Figure 2 averaging 25 μm in diameter on one side and 35 μm in diameter on the other side of 25-μm-thick films. Porosity was estimated at 26% using an average hole diameter. The micromachined contactors were coated with Teflon to make them more nonwetting to water, giving higher breakthrough pressures.

The Gelman 3-μm Zefluor Teflon membrane has a microporous 15-μm-thick Teflon layer mounted onto a Teflon macroporous substrate measured at 165 μm thick, for a total thickness of 180 μm. The porosity of the 15-μm microporous layer is calculated to be 44%, based on void volume information obtained from Gelman. The contactor device was consistently configured with the Teflon layer located toward the organic liquid side for all experiments.

The microcontactor channels are 10 cm long, 1 cm wide, and can be configured with various channel heights that can be different for the feed and solvent sides. In all experiments reported here, the same channel heights were used on both sides and at equal flow rates. Channel heights of 200, 300, 400, and 500 μm were used. The micromachined contactor plates have 8 cm of active porous area, while the full 10 cm of channel length is utilized with the microporous Teflon membrane. A Harvard Apparatus, Model No. 22, syringe infusion pump was used to transfer the liquids at a constant flow rate through the contactor. The pressure differential between the two liquid streams was measured in the tubing immediately downstream of the discharge ports of the microcontactor device

using a water manometer. The discharge pressure of the water stream was kept slightly higher than the cyclohexane stream discharge pressure, but the difference in pressures was generally less than 1 in. of water column.

RESULTS AND DISCUSSION

The equilibrium partitioning data are presented in Table 1. Within the accuracy of the measurements, the partition coefficient is fairly constant over the range of total concentrations examined. An equilibrium partition coefficient of 1.3 is used in subsequent theoretical calculations.

Cyclohexane and water were contacted in the microchannel devices in the absence of cyclohexanol, as described above, and the water effluent was analyzed for cyclohexane concentration. This experiment was performed using both the micromachined contactor plate and the commercial microporous Teflon membrane at varying channel heights and flow rates. The dominant mass transfer resistance in these experiments is diffusion in the feed-side flow channel. Therefore, the theoretical model was solved for the feed-side channel only, with the boundary condition at the contactor plate [Equation (8)] changed to a constant concentration equal to the saturation concentration of cyclohexane in water; saturation is 58 mg/L (19). Here, concentrations were nondimensionalized by the saturation concentration. The diffusivity of cyclohexane in water is 0.84×10^{-5} cm^2/s (19).

The results of contacting water and cyclohexane are summarized in Figure 6. The results for the microporous Teflon membrane show good agreement with theoretical predictions. A contact length of 8 cm was used in the calculations, which is appropriate for the micromachined plates. However, the Teflon membrane utilizes the full 10 cm of the channel length, which accounts for actual performance exceeding predicted performance. The micromachined contactor

TABLE 1. EQUILIBRIUM DISTRIBUTION COEFFICIENT FOR CYCLOHEXANOL PARTITIONING BETWEEN WATER AND CYCLOHEXANE, MEASURED FOR A RANGE OF TOTAL SOLUTE CONCENTRATIONS

Total $C_6H_{11}OH$ concentration [a] (mg/L)	Conc. ratio water/organic day 1	Conc. ratio water/organic day 2
44	1.69	1.29
86	1.30	0.98
154	1.30	0.70
307	1.09	0.88
464	1.21	0.78
620	1.11	2.13
779	0.82	1.20
843	0.69	2.16
883	0.43	1.62
Average	**1.07**	**1.30**

[a] Calculated as total mass of cyclohexanol divided by the total volume of both liquid phases.

plate shows poorer mass transfer efficiency in these particular experiments. This decreased efficiency can be explained by microstructural differences. The cyclohexane more fully wets the microporous Teflon membrane providing thorough contact of the two liquids. In contrast, the micromachined membrane has holes drilled through a solid substrate, so there is less area for direct contact between the liquids. Mathematically, the assumption of uniform saturation along the contactor plate as a boundary condition is not strictly valid. The increased scatter in the data at residence times greater than 2 min and the lower effluent concentrations are attributed to volatility losses of cyclohexane in the longer experiments.

Figure 6 also illustrates the importance of minimizing channel height to enhance mass transfer, a key advantage of microchannel devices. Reducing the

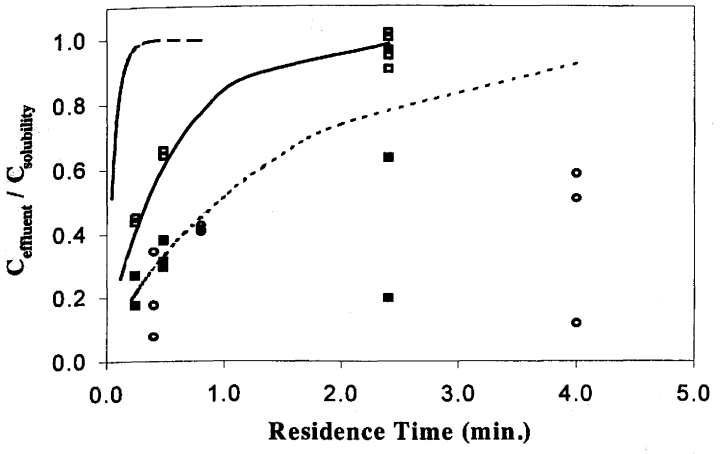

FIGURE 6. Effluent concentration of cyclohexane in water after contacting liquid cyclohexane in microchannel devices for various channel heights and flow rates using both micromachined contactor (MMC) plates and microporous Teflon membranes (Tef), including 300-μm channel heights with Tef (❐), 500-μm channel heights with Tef (○), and 300-μm channel heights with MMC plate (■). Experimental data are compared with theoretical prediction for 8-cm by 1-cm flow channels and 100-μm channel heights (— —), 300-μm channel heights (—), and 500-μm channel heights (- - -).

channel height from 500 μm to 100 μm causes the residence time required to approach equilibrium to decrease from minutes to a fraction of a minute, thereby permitting much higher throughput per unit system hardware volume. The dramatic advantage occurs because the mass transfer rate is proportional to the diffusion coefficient and inversely proportional to the square of the characteristic distance—the channel height in this case. This can be seen by normalizing the abscissa in Figure 6 by multiplying by the diffusion coefficient and dividing by the square of the channel height, which causes the theoretical curves to overlay. Future work will be directed toward decreasing flow channel heights in experimental devices to 100 μm or less.

Solvent extraction data acquired with cyclohexanol as the extractant are summarized in Figure 7, which illustrates the relative importance of channel height to overall mass transfer efficiency by allowing comparison of data obtained for three channel heights using the commercial Teflon membrane. In addition, data for one channel height using the micromachined contactor plate are also shown in Figure 7. Data for each contactor and channel height were acquired from a single run by varying the flow rate, with several purge volumes between conditions to allow the system to equilibrate.

The Teflon membrane tests showed a significant improvement in performance when the flow channel heights were decreased from 400 μm to 300 μm, indicating appreciable mass transfer resistance in the flow channels at 400-μm channels. However, no discernible improvement was seen in decreasing the channel heights further to 200 μm, indicating that the mass transfer resistance in the membrane dominates at this smaller channel height. The micromachined contactor plate performs at least as well as the commercial Teflon membrane.

The data for the 300-μm channel height are compared with theoretical calculations in Figure 8. The equilibrium distribution coefficient is set to the average measured value of 1.3, and the interface mass transfer resistance is neglected by setting the Sherwood number to a low value (0.0003). Different theoretical curves are shown for values of the plate effective diffusion coefficient. None of these curves fit the data well over the full range of residence times. The relatively poor fit suggests that the equilibrium partition coefficient is too low and a value approaching 2 would fit the data better. However, this higher value would also require the effective diffusion coefficient through the contactor plate to be near the bulk-phase diffusion coefficient, which is not indicated by the comparisons between various channel heights as discussed above. Another possible cause for this discrepancy is the concentration dependence of the equilibrium partition coefficient, which so far has not been elucidated by the

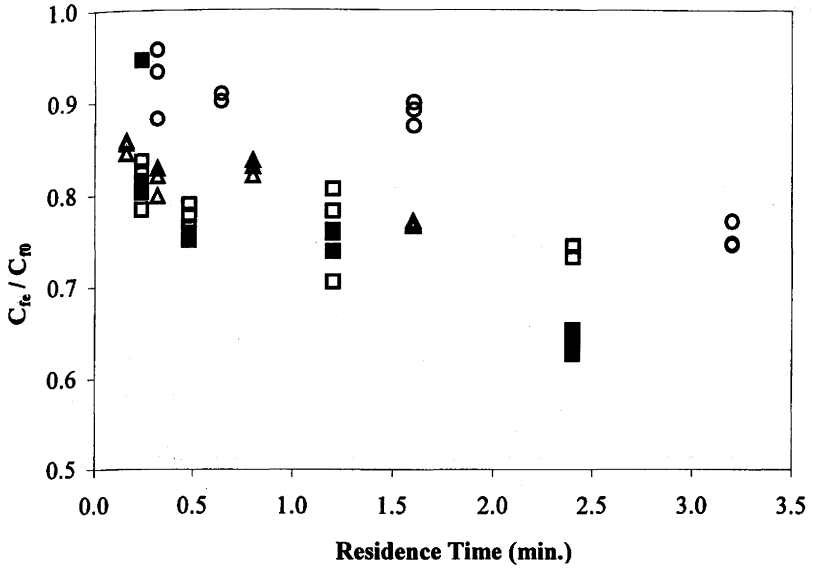

FIGURE 7. Summary of solvent extraction data presented as effluent cyclohexanol concentration normalized by feed concentration for both micromachined contactor (MMC) plates and microporous Teflon membranes (Tef), including 200-μm channel heights with Tef (△), 300-μm channel heights with Tef (❐), 400-μm channel heights with Tef (○), and 300-μm channel heights with MMC plate (■).

partitioning data. Another concern involves nonuniformities in the flow distribution due to variations in channel height caused by flexing of the contactor plates and membranes, which cannot be captured in the two-dimensional theoretical model. Variations in channel heights effectively allow bypass of the device because a disproportionate fraction of the flow will follow the thicker paths that have more mass transfer resistance, thereby giving poorer overall mass transfer.

Assuming that the theoretical curves are indicative of mass transfer resistance through the contactor plate and considering the longer residence time data, the

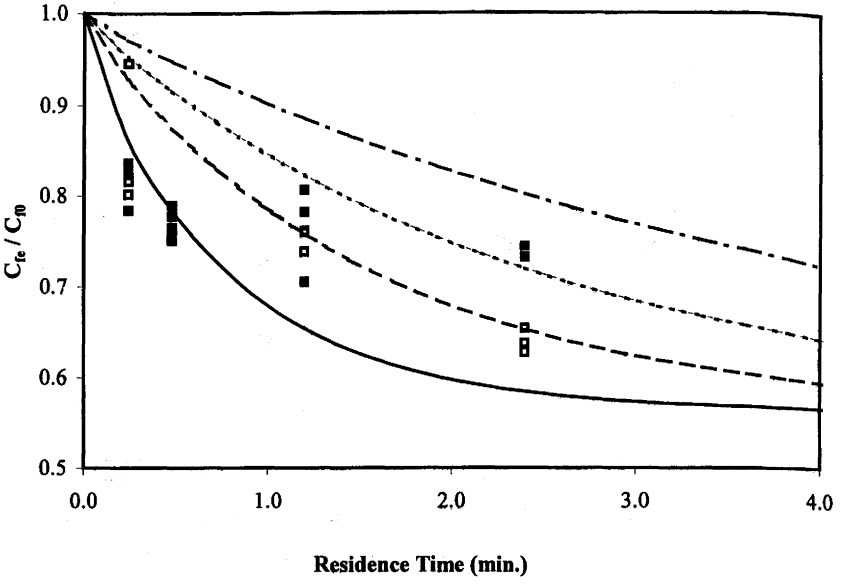

FIGURE 8. Comparison of solvent extraction data for 300-μm channels with theoretical prediction, presented as effluent cyclohexanol concentration normalized by feed concentration; 300-μm channel heights with Teflon membrane (❐) and 300-μm channel heights with micromachined plate (■) compared with predictions for $D_e/D_f = 1.0$ (—), $D_e/D_f = 0.1$ (— —), $D_e/D_f = 0.05$ (- - -), and $D_e/D_f = 0.025$ (— - —), using 1-cm by 8-cm channel dimensions, $m_s = 1.3$, $h_f = 25$ μm, $D_f = D_s = 0.84 \times 10^{-5}$ cm^2/s, and neglecting mass transfer resistance at the interface.

micromachined contactor plate has an effective diffusion coefficient that is approximately one-tenth of the bulk-phase diffusion coefficient. A factor of 4 can be attributed to the 26% porosity. Tortuosity is not expected to be important because the holes are straight and close to vertical. The additional 2.5 factor may be attributed to poor flow distribution or to inactive pores if bubbles are trapped in the pores, as two examples.

The Teflon membrane is approximately seven times thicker than the micromachined contactor plate, so the effective diffusion coefficient must be

scaled accordingly. Therefore, the effective diffusion coefficient displayed by the long-residence-time Teflon membrane data would be closer to one-third, which is considerably larger than the micromachined membrane. This illustrates that there are multiple avenues to improving mass transfer through the contactor plate, including increasing the porosity and making the plate thinner. Other concepts are being evaluated as well.

CONCLUSIONS

Microchannel devices offer a novel approach to chemical processing where very rapid heat and mass transfer are achieved, thereby realizing high throughput per unit system volume, more effective process control, and better efficiencies. Furthermore, fabrication techniques adapted from the microelectronics industry can provide economies of mass production to support process scaleup, instead of relying on traditional economies of scale.

The performance of a microchannel device has been demonstrated using both micromachined contactor plates and commercial microporous membranes over a range of flow rates and channel heights. Results indicate that first-generation micromachined contactor plates perform at least as well as the commercial membranes tested, with significant potential for improving performance. Future efforts in developing micromachined plates will be directed toward reducing mass transfer resistance by reducing plate thickness, increasing porosity, and using more rigid materials to give uniform flow distribution.

Overall mass transfer in microchannel devices can be limited by diffusion in the flow channels, by diffusion through the contactor plate, or by the interface. Theoretical predictions and comparison of data for varying channel heights indicate that contactor-plate mass transfer becomes limiting as the channel height decreases below 300 μm for current contactor plates. However, as the contactor

plates become more efficient, the need is anticipated for operating with substantially smaller channel heights. Therefore, continued advancements in this technology will require efforts in reducing the mass transfer resistance of both the contactor plates and the flow channels.

ACKNOWLEDGMENTS

This project was funded by the Pacific Northwest National Laboratory's Laboratory Directed Research and Development (LDRD) program, which is supported by the U.S. Department of Energy under contract DE-AC06-76RLO 1830.

REFERENCES

1. R. S.Wegeng, C. J. Call, and M. K. Drost, Chemical System Miniaturization, PNNL-SA-27317, Pacific Northwest National Laboratory, Richland, Washington, 1996.
2. E. Harvey, P. Rumsby, M. Gower, and J. Remnant, "Microstructuring by Excimer Laser," in *Proceedings of the SPIE Conference on Micromachining and Microfabrication Process Technology*, 1995.
3. M. Bowers and I. Mudawar, "High Flux Boiling in Low Flow Rate, Low Pressure Drop Mini-Channel and Micro-Channel Heat Sinks," Int. J. Heat Mass Trans. *3*, 321–332 (1993).
4. M. Kleiner, K. Stefan, and K. Haberger, "High Performance Forced Air Cooling Scheme Employing Microchannel Heat Exchangers," in *MicroSim 95*, Southampton, September 1995.
5. J. Cuta, W. Bennett, and C. McDonald, "Fabrication and Testing of

Microchannel Heat Exchangers," in *Proceedings of the SPIE Conference on Micromachining and Microfabrication Process Technology*, 1995.

6. W. Ehrfield, V. Hessel, H. Mobius, T. Richter, and K. Russow, "Potentials and Realization of Microreactors," presented at the DECHEMA Workshop on Microsystem Technology for Chemical and Biological Microreactors, February 1995.
7. E. Becker, "Development of the Separation Nozzle Process for Enrichment of Uranium," Ger. Chem. Eng. *9*, 204–208 (1986).
8. M. Zbedlick, R. Anderson, J. Jankowski, B. Kline-Schoder, L. Christel, R. Miles, and W. Weber, "Thermopneumatically Actuated Microvalves and Integrated Electro-Fluidic Circuits," presented at the Solid-State Sensor and Actuator Workshop, 1994.
9. P. Barth, C. Beatty, L. Field, J. Baker, and G. Gordon, "A Robust Normally Closed Silicon Microvalve," presented at the Solid-State Sensor and Actuator Workshop, 1994.
10. C. Friedrich and B. Kikkeri, "Rapid Fabrication of Molds by Mechanical Micromilling: Process Development," in *Proceedings of the SPIE Conference on Micromachining and Microfabrication Process Technology*, 1995.
11. J. Arnold, U. Dasbach, W. Ehrfeld, K. Hesch, and H. Lowe, "Combination of Excimer Laser Micromachining and Replication Processes Suited for Large-Scale Production (Laser-LIGA)," presented at the EMRS Spring Meeting, Strasbourg, France, May 1994.
12. R. A. Leonard, D. B. Chamberlain, and C. Conner, "Centrifugal Contactors for Laboratory-Scale Solvent Extraction Tests," Sep. Sci. Technol. *32*(1-4), 193–210 (1997).
13. H. R. C. Pratt, "Interphase Mass Transfer," in *Handbook of Solvent Extraction*, T. C. Lo, M. H. I. Baird, and C. Hanson, Eds., John Wiley and Sons, Inc., New York, 1983.

14. R. G. Holmes, A. J. Bull, A. M. Simper, J. E. A. Shaw, D. E. Brennan, R. E. Turner, R. I. Simpson, and L. Westwood, Method and Apparatus for Diffusive Transfer Between Immiscible Fluids, International Patent WO 96/12541, May 1996.
15. A. F. Sieber and J. R. Fair, "Scale-up of Hollow Fiber Extractors," Sep. Sci. Technol. *32*(1-4), 573–583 (1997).
16. R. Prasad and K. K. Sirkar, "Membrane-Based Solvent Extraction," in *Membrane Handbook*, W. S. Winston Ho and K. K. Sirkar, Eds., Chapman & Hall, New York, 1992.
17. M. Cox and D. S. Flett, "Metal Extractant Chemistry," in *Membrane Handbook*, W. S. Winston Ho and K. K. Sirkar, Eds., Chapman & Hall, New York, 1992.
18. J. Crank, *The Mathematics of Diffusion*, Second Edition, Oxford University Press, New York, 1975.
19. D. R. Lide, Ed., *CRC Handbook of Chemistry and Physics*, 75th Edition, CRC Press, Ann Arbor, Michigan, 1994.